RESEARCH ARTICLE

A learning-based approach for autonomous outage detection and coverage optimization

Ahmed Zoha[1]*, Arsalan Saeed[2], Ali Imran[3], Muhammad Ali Imran[2] and Adnan Abu-Dayya[1]

[1] QMIC, Qatar Science and Technology Park, Doha, 210531, Qatar
[2] ICS, University of Surrey, Guildford, GU2 7XH, UK
[3] University of Oklahoma, Tulsa, 71435, USA

ABSTRACT

To be able to provide uninterrupted high quality of experience to the subscribers, operators must ensure high reliability of their networks while aiming for zero downtime. With the growing complexity of the networks, there exists unprecedented challenges in network optimization and planning, especially activities such as cell outage detection (COD) and mitigation that are labour-intensive and costly. In this paper, we address the challenge of autonomous COD and cell outage compensation in self-organising networks (SON). COD is a pre-requisite to trigger fully automated self-healing recovery actions following cell outages or network failures. A special case of cell outage, referred to as sleeping cell, remains particularly challenging to detect in state-of-the-art SON, because it triggers no alarms for operation and maintenance entity. Consequently, no SON compensation function can be launched unless site visits or drive tests are performed, or complaints are received by affected customers. To address this issue, our COD solution leverages minimization of drive test functionality, recently specified in third generation partnership project Release 10 for LTE networks, in conjunction with state-of-the-art machine learning methods. Subsequently, the proposed cell outage compensation mechanism utilises fuzzy-based reinforcement learning mechanism to fill the coverage gap and improve the quality of service, for the users in the identified outage zone, by reconfiguring the antenna and power parameters of the neighbouring cells. The simulation results show that the proposed framework can detect cell outage situations in an autonomous fashion and also compensate for the detected outage in a reliable manner. Copyright © 2015 John Wiley & Sons, Ltd.

*Correspondence

A. Zoha, QMIC, Qatar Science and Technology Park, Doha, 210531, Qatar.
E-mail: ahmedz@qmic.com

1. INTRODUCTION

The increased demands of high throughput, coverage and end user quality of service requirements, driven by ever increasing mobile usage, incur additional challenges for the network operators. Fueled by the mounting pressure to reduce capital and operational expenditures and improve efficiency in legacy networks, the self-organising network (SON) paradigm aims to replace the classic manual configuration, post deployment optimization and maintenance in cellular networks with self-configuration, self-optimization and self-healing functionalities. A detailed review of the state-of-the-art SON functions for legacy cellular networks can be found in [1]. The main task within self-healing functional domain is autonomous cell outage detection (COD) and compensation. Current SON solutions generally assume that the spatio-temporal knowledge of a problem that requires SON-based compensation is fully or at least partially available; for example, location of cover-age holes, handover ping-pong zones or congestion spots are assumed to be known by the SON engine. Traditionally, to assess and monitor mobile network performance, manual drive test has to be conducted. However, this approach cannot deliver the stringent resource efficiency and low latency and cannot be used to construct dynamic models to predict system behaviour in live-operation fashion.

This is particularly true for a *sleeping cell* (SC) scenario, which is a special case of cell outage that can remain undetected and uncompensated for hours or even days, because no alarm is triggered for operation and maintenance system [2]. An SC either cause deterioration of the service level or a total loss of radio service in its coverage area, due to a possible software, firmware or hardware problem. SC can only be detected by means of manual drive tests or via subscriber complaints. These solutions are not only time and resource consuming but also require expert knowledge to troubleshoot the problem. As future cellular network has to rely more and more on higher cell densities, manual

or semi-manual detection of SC can become a huge challenge. Therefore, automatic cell detection has become a necessity so that timely compensation actions can be triggered to resolve any issues. Once the outage is detected, the operator can achieve self-resilience to network outages by employing intelligent self-healing mechanism.

Self-healing block in SON consists of two modules, namely COD and cell outage compensation (COC). COD aims to autonomously detect outage cells, that is, cells that are not operating properly due to possible failures, for example, external failure such as power supply or network connectivity, or even misconfiguration [2–4]. On the other hand, COC refers to the automatic mitigation of the degradation effect of the outage by appropriately adjusting suitable radio parameters, such as the pilot power, antenna elevation and azimuth angles of the surrounding cells for coverage optimization [2].

The reported studies in literature that addressed the problem of COD are either based on quantitative models [5], which requires domain expert knowledge, or simply rely on performance deviation metrics [6]. Until recently, researchers have applied methods from the machine learning domain such as clustering algorithms [7] as well as Bayesian networks [8] to automate the detection of faulty cell behaviour. Coluccia et al. [9] analysed the variations in the traffic profiles for 3G cellular systems to detect real-world traffic anomalies. In particular, the problem of SC detection has been addressed by constructing and comparing a visibility graph of the network using *neighbour cell list* reports [3].

Compared with the aforementioned approaches, the COD solution proposed in this paper differs in various aspects. Our proposed COD framework adopts a model-driven approach that makes use of mobile terminal-assisted data gathering solution based on minimise drive testing (MDT) functionality [2] as specified by third generation partnership project (3GPP). MDT functionality allows e-utran Node B (eNB) to request and configure user equipment (UE) to report back the key performance indicators (KPIs) from the serving and neighbouring cells along with their location information. To accurately capture the network dynamics, we first collect UE reported MDT measurements and further extract a minimalistic KPI representation by projecting them to a low-dimensional embedding space. We then employ these embedded measurements together with density and domain-based anomaly detection models namely *local outlier factor-based detector* (LOFD) and *one-class support vector machine-based detector* (OCSVMD). We compare and evaluate the performance of these learning algorithms to autonomously learn the 'normal' operational profile of the network, while taking into consideration the acute dynamics of the wireless environment due to channel conditions as well as load fluctuations. The learned profile leverages the intrinsic characteristics of embedded network measurements to intelligently diagnose a sleeping/outage cell situation. To the best of our knowledge, no prior study examines the use of OCSVMD and LOFD in conjunction

with embedded MDT measurements for autonomous COD. This is in contrast to state-of-the-art techniques that analyse one or two KPIs to learn the decision threshold levels and subsequently apply them for detecting network anomalies. In addition, the COD framework further exploits the geo-location associated with each measurement to localise the position of the faulty cell, enabling the SON to autonomously trigger COC actions.

Once the outage is properly detected, an automatic COC scheme is required for coverage optimization in order to continue serving the UEs in the outage area. Considering the acute dynamics of the always varying wireless environment in general, and the high variability in terms of load fluctuations, in dense wireless deployments, we propose a fuzzy logic-based reinforcement learning (RL) algorithm, which allows to learn online, through interactions with the surrounding environment, the best possible policy to compensate the outage. In literature, fuzzy logic algorithm has been studied [10] to address the problem of self-recovery in case of cell outage in Long Term Evolution (LTE) network. Moreover, fractional power control-based approaches in conjunction with RL algorithm [11] have also been studied to address the problem of near far effect by controlling the required signal-to-interference-plus-noise ratio (SINR), in order to reduce the call blocking rate. Motivated by this, partnership project (3GPP we propose a fuzzy RL-based compensation scheme in order to minimise the interference caused by the compensating sites.

The main contribution of this paper can be summarised as follows: firstly, we propose a novel COD framework that exploits recently introduced MDT functionality in conjunction with state-of-the-art machine learning methods to detect and localise cell outages in an autonomous fashion. Secondly, we demonstrate the applicability of a fuzzy RL-based method to achieve autonomous self-recovery in case of network outages. Finally, the proposed solution is validated with simulations that are set up in accordance with 3GPP LTE standards. The remainder of this paper is structured as follows: Section 2 presents the system architecture for proposed self-healing framework. Section 3 provides a detailed discussion of COD framework that also includes a brief description of LOFD and OCSVMD techniques that are used to profile, detect and localise anomalous network behaviour. In Section 4, the COC scheme has been explained, whereas in Section 5, we provide details of our simulation setup and evaluation methodology. Furthermore, we present extensive simulation results to substantiate the performance of our proposed self-healing framework. Finally, Section 6 concludes this paper.

2. SYSTEM DESIGN

To alleviate the network performance deterioration, the first step is to detect the cell/base station (BS) in outage. This can be achieved by monitoring deviations from the
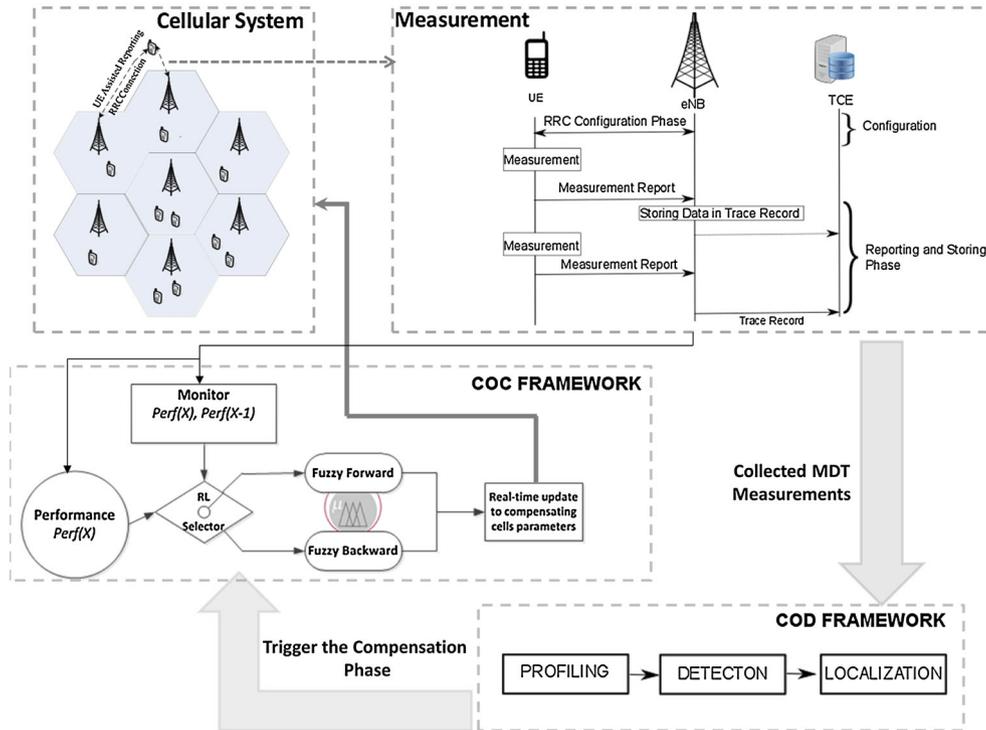
Figure 1. System model for autonomous COD and COC framework.

KPI measurement report of the fault-free network. Thereafter, the parameters of BSs neighbouring the outage BS can be adjusted according to the operators policy so as to compensate for the outage situation. Hence, we propose a self-healing framework that primarily consists of the COD and COC stages, as illustrated in Figure 1.

COD stage: As shown in Figure 1, firstly, to profile the normal operational behaviour of the network, our solution collects KPIs from the network leveraging MDT functionality. The goal is to use the learned profile to perform problem identification and localization autonomously, during the monitoring period.

The MDT reporting schemes have been defined in LTE Release 10 during 2011 [2]. The release proposes to construct a database of MDT reports from the network using *Immediate* or *Logged* MDT reporting configuration. In this study, the UEs are configured to report the cell identification and radio-measurement data to the target eNB based on immediate MDT configuration procedure as shown in Figure 1. The signalling flow of MDT reporting procedure consists of configuration, measurement, reporting and storing phase. In order to collect measurements, the UE is configured for event-based periodical reporting. It is to be noted that immediate MDT procedure can be configured to start periodical reporting, once a trigger condition is met. In our simulation setup, periodic measurements are performed once an A2 event (i.e. serving cell becomes worst than a threshold) occurs and subsequently triggers the UEs to report periodic measurements from the problematic coverage area. The KPI measurements consist of serving

Table I. MDT reported measurements.

Measurements	Description
Location	Longitude and latitude information
Serving cell info	Cell global identity
RSRP	Reference signal received power in dBm
RSRQ	Reference signal received quality in dB
Neighbouring cell information	Three strongest intra-LTE RSRP, RSRQ information

and neighbours reference signal received power (RSRP), serving and neighbours reference signal received quality (RSRQ), as specified in Table I, that is further reported to the serving eNB. The eNB after retrieving these measurements further appends time and wide-band channel quality information (CQI) and forwards it to trace collection entity. Trace collection entity collects and stores the trace reports that are subsequently processed to construct an MDT database. In this study, the trace records obtained from the reference scenario (i.e. fault-free) act as a benchmark data and are used by the anomaly detection models to learn the network profile. These models are then employed to autonomously detect and localise outage situations. The proposed COD framework as shown in Figure 1 consists of profiling, detection and localization phases, which is further discussed in Section 3.

COC stage: Once the cell outage situation has been detected by the operation and maintenance, subsequently, a COC scheme is triggered to optimise the coverage and capacity of the identified outage zone according to the operator policies. This is achieved by adjusting the antenna gain through down-tilt and the downlink transmission power of the potential compensating eNBs. In our proposed framework, COC is implemented via a fuzzy logic-based RL scheme, as illustrated in Figure 1, which is further explained in Section 4.

3. CELL OUTAGE DETECTION FRAMEWORK

The proposed COD framework consists of profiling, detection and localization phases that are subsequently discussed in detail.

3.1. Profiling phase

In the profiling phase, the trace records are processed to extract the feature vector $\mathbf{O}$ corresponding to each MDT measurement. The measurements including RSRP and quality of the serving, as well as of the three strongest neighbouring cells and the CQI, are concatenated into a feature vector, $\mathbf{O}$, which is expressed as follows:

$$\mathbf{O} = [RSRP_S, RSRP_{n1}, RSRP_{n2}, RSRP_{n3}, RSRQ_S, \\ RSRQ_{n1}, RSRQ_{n2}, RSRQ_{n3}, CQI] \quad (1)$$

where the subscripts S and n denote the serving and neighbouring cells, respectively. The observation vector, $\mathbf{O}$, is a nine-dimensional feature vector of numerical features that corresponds to one network measurement. To reduce the complexity of storage, processing and analysing this nine-dimensional feature vector is further embedded to three dimensions in the Euclidean space using Multi-dimensional Scaling (MDS) method [12]. MDS provides a low dimensional embedding of the target KPI vectors $\mathbf{O}$ while preserving the pairwise distances amongst them. Given a $t \times t$ dissimilarity matrix $\Delta^{\mathbf{X}}$ of the MDT dataset, MDS attempts to find t data points $\psi_1, \ldots, \psi_t$ in m dimensions, such that Δ^{Ψ} is similar to $\Delta^{\mathbf{X}}$. Classical MDS operates in Euclidean space and minimises the following objective function

$$\min_{\psi} \sum_{i=1}^{t} \sum_{j=1}^{t} \left(\phi_{ij}^{(X)} - \phi_{ij}^{(\Psi)} \right)^2 \quad (2)$$

where $\phi_{ij}^{(X)} = \|x_i - x_j\|^2$ and $\phi_{ij}^{(\Psi)} = \|\psi_i - \psi_j\|^2$. Equation (2) can be reduced to a simplified form by representing $\Delta^{\mathbf{X}}$ in terms of a kernel matrix using

$$\mathbf{X}^T\mathbf{X} = -\frac{1}{2}\mathbf{H}\Delta^{\mathbf{X}}\mathbf{H} \quad (3)$$

where $\mathbf{H} = \mathbf{I} - \frac{1}{t}\mathbf{e}\mathbf{e}^T$ and $\mathbf{e}$ is a column vector of all 1's. Hence, (2) can be rewritten as

$$\min_{\psi} \sum_{i=1}^{t} \sum_{j=1}^{t} \left(x_i^T x_j - \psi_i^T \psi_j \right)^2 \quad (4)$$

As shown in [12], that Ψ can be obtained by solving $\Psi = \sqrt{\Lambda}\mathbf{V}^T$, where $\mathbf{V}$ and Λ are the matrices of top m eigenvectors and their corresponding eigenvalues of $\mathbf{X}^T\mathbf{X}$, respectively. The m dimensional embeddings of the data points are the rows of $\sqrt{\Lambda}\mathbf{V}^T$, whereas the value of m is chosen to be 3 in our case. Equation (4) represents the fact that MDS minimises the Euclidean distances between distance matrices of the original and embedded space (i.e. $\Delta^{\mathbf{X}}$ and Δ^{Ψ}, respectively). MDS aims to achieve an optimal spatial configuration such that distances in the new configuration (i.e. $\phi_{ij}^{(\Psi)}$) are close in value to the observed distances (i.e. $\phi_{ij}^{(X)}$). This is achieved by constructing a configuration of t points in Euclidean space by using information about the distances between the t patterns in m dimensions. The MDS-based pre-processing of the network observation $\mathbf{O}^e$ has several advantages. In literature, MDS technique has been widely used as a dimensionality reduction method [12] to transform high-dimensional data into meaningful representation of reduced dimensionality. One of the problems with high-dimensional datasets is that in many cases, not all of the measured variables are 'critical' for understanding the underlying phenomena. As shown in literature that dimensionality reduction is a critical pre-processing step for the analysis of real-world datasets, because it mitigates the curse of dimensionality and other undesired properties of high-dimensional spaces. The low-dimensional embedding helps to reveal a hidden structure that is not obvious from raw data matrices, allowing to explore the interrelationships of high-dimensional spaces. Given the growing complexity of the networks, particularly in case of SON, it is challenging to identify few measurements that can accurately capture the behaviour of the system. The MDS pre-processing of the network measurements allows to achieve reduced representation that corresponds to intrinsic dimensionality of data. Consequently, it facilitates data modelling and further allows the anomaly detection algorithms to obtain better estimation of data density. As a result, the anomalous network measurements can be detected with higher accuracy, as discussed in the succeeding text. Moreover, unlike other dimensionality reduction methods such as principal component analysis or linear discriminant analysis, MDS does not make an assumption of linear relationships between the variables, and hence applicable to wide variety of data.

In addition to network measurements, each MDT report is tagged with the location and time information as listed in Table I, which is used in conjunction with RSRP values to estimate the dominance or the coverage area of target BS in the network. The dominance map estimation is further used to autonomously localise the position of the outage BS.
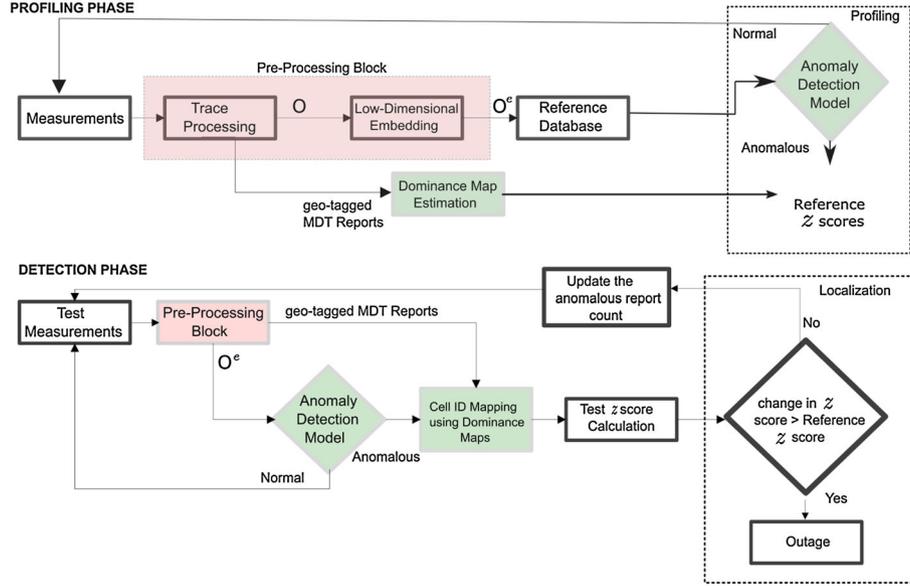
Figure 2. An overview of profiling and detection phases in COD framework.

The next step after the pre-processing is to develop a reference database, $\mathbf{D}_M$, by storing the embedded measurements that represent the normal operation of the network. As shown in Figure 2, this reference database is used by the state-of-the-art anomaly detection algorithms to learn the 'normal' network profile. The goal of these algorithms is to define an anomaly detection rule that can differentiate between normal and abnormal MDT measurements by computing a threshold 'φ' based on a dissimilarity measure '$\mathcal{D}$'. Thus, it can be treated as a binary classification problem that can formally be expressed as follows:

$$f(x_i) = \begin{cases} \text{Normal}, & \text{if } \mathcal{D}(x_i, \mathbf{D}_M) \leqslant \varphi \\ \text{Anomalous}, & \text{if } \mathcal{D}(x_i, \mathbf{D}_M) > \varphi \end{cases} \quad (5)$$

Two state-of-the-art anomaly detection algorithms, OCSVMD and LOFD, are examined for modelling the dynamics of network operational behaviour. The brief working description of the two detection algorithms are summarised as follows.

3.1.1. Local outlier factor-based detector.

The LOFD method [13] adopts a density-based approach to measure the degree of outlyingness of each instance. In comparison with nearest neighbour-based approaches, it works by considering the difference in the local density ρ of the sample to that of its k neighbours, instead of relying on distance estimation alone. A higher score will be assigned to the sample, if ρ is highly different from the local densities of its neighbour. The algorithm starts by first computing the distance of the measurement x to its kth nearest neighbour denoted by d_k, such that

$$\begin{aligned} d(x, x_j) &\leqslant d(x, x_i) \text{ for at least } k \text{ samples} \\ d(x, x_j) &< d(x, x_i) \text{ for at most } k-1 \text{ samples} \end{aligned} \quad (6)$$

The subsequent step is to construct a neighbourhood $\mathcal{N}_k(x)$ by including all those points that fall within the d_k value. The following step is to calculate the reachability distance of sample x with respect to the rest of the samples

$$d_r(x, x_i) = \max\{d_k(x_i), d(x, x_i)\} \quad (7)$$

The local reachability density ρ is the inverse of average d_r and can be defined as

$$\rho(x) = \frac{|\mathcal{N}_k(x)|}{\sum_{x_i \in \mathcal{N}_k(x)} d_r(x, x_i)} \quad (8)$$

Finally, the $\mathcal{S}^{(LOFD)}$ represents a local density-estimation score, whereas value close to 1 mean x_i has same density relative to its neighbours. On the other hand, a significantly high $\mathcal{S}^{(LOFD)}$ score is an indication of anomaly. It can be computed as follows:

Algorithm 1 Local Outlier Factor Based Detection Model

1: Input Data $\mathcal{X} = \{x_j\}_{j=1}^N$, k_{min}, k_{max}
2: **for** $j = 1, 2, \ldots, N$: **do**
3:    **for** $k = k_{min}$ to k_{max}: **do**
4:      Find $d_k(x_j)$ from Equation 6
5:      Find the neighbourhood $\mathcal{N}_k$ of x_j
6:      Calculate $d_r(x_j, x_i)$ from Equation 7
7:      Calculate $\rho(x_i)$ from Equation 8
8:      Calculate $\mathcal{S}^{(LOFD)}$ from Equation 9
9:    **end for**
10:   $\mathcal{S}^{(LOFD)} = \max(\mathcal{S}^{(LOFD)}{}_{k_{min}}, \ldots, \mathcal{S}^{(LOFD)}_{k_{max}})$
11: **end for**

$$\mathcal{S}^{(LOFD)}(x) = \frac{\sum_{x_i \in \mathcal{N}_k(x)} \frac{\rho(x_i)}{\rho(x)}}{\mid \mathcal{N}_k(x) \mid} \qquad (9)$$

Because $\mathcal{S}^{(LOFD)}$ is sensitive to the choice of k, we iterate between k_{min} and k_{max} value for each sample and take the maximum $\mathcal{S}^{(LOFD)}$ as described in Algorithm 1.

3.1.2. One-class support vector machine-based detector.

One-class support vector machine (SVM) by Schölkopf et al. [14] maps the input data/feature vectors into a higher dimensional space in order to find a maximum margin hyperplane that best separates the vectors from the origin. The idea is to find a binary function or a decision boundary that corresponds to a classification rule

$$f(x) = <\mathbf{w}, \mathbf{x}> + b \qquad (10)$$

The $\mathbf{w}$ is a normal vector perpendicular to the hyperplane, and $\frac{b}{\|\mathbf{w}\|}$ is an offset from the origin. For linearly separable cases, the maximisation of margin between two parallel hyperplanes can be achieved by optimally selecting the values of w and b. This margin, according to the definition, is $\frac{2}{\|\mathbf{w}\|}$. Hence, the optimal hyperplane should satisfy the following conditions

$$minimise \; \frac{1}{2}\|\mathbf{w}\|^2$$
$$subject \; to : y_i(\langle \mathbf{w}, x_i \rangle + b) \geqslant 1 \qquad (11)$$
$$for \; i = 1, \ldots, N$$

The solution of the optimization problem can be written in an unconstrained dual form, which reveals that the final solution can be obtained in terms of training vectors that lie close to the hyperplanes, also referred to as support vectors. To avoid overfitting on the training data, the concept of *soft decision* boundaries was proposed, and slack variable ξ_i and regularisation constant ν are introduced in the objective function. The slack variable is used to soften the decision boundaries, while ν controls the degree of penalization of ξ_i. Few training errors are permitted if ν is increased while degrading the generalisation capability of the classifier. A *hard margin* SVM classifier is obtained by setting the value of $\nu = \infty$ and $\xi = 0$. The detail mathematical formulation for SVM models can be found in [14]. The original formulation of SVM is for linear classification problems; however, non-linear cases can be solved by applying a kernel trick. This involves replacing every inner product of $x.y$ by a non-linear kernel function, allowing the formation of non-linear decision boundaries. The possible choices of kernel functions includes polynomial, Gaussian radial basis function (RBF) and sigmoid. In this study, we have used the RBF kernel, $\kappa(x, y) = exp(-\|x - y\|^2/2\sigma^2)$, and the corresponding parameter values of the model are selected using cross-validation (CV) method, as described in Algorithm 2.

As shown in Figure 2, using the benchmark data, we compute a reference z-score for each target eNB in the network. The z-score is calculated as follows: $z_b = \frac{|n_b - \mu_n|}{\sigma_n}$ where n_b is the number of MDT reports labelled as anomalies for the eNB b, and variables μ_n and σ_n are the mean and standard deviation anomaly scores of the neighbouring cells. In the profiling phase, we also estimate the so-called dominance area, that is, for each cell, we define the area where its signal is the strongest. This is to establish the coverage range for each cell by exploiting the location information tagged with each UE measurement. The dominance estimation is required to determine the correct cell and its corresponding MDT measurement association during an outage situation. This is because as soon as the SC situation develops in the network, the malfunctioning eNB either becomes completely unavailable or experience severe performance issues. As a result UEs in the affected area experience frequent handovers to the neighbouring cells. Hence, the reported measurements contain the cell global identity of the neighbouring cells, instead that of the target cell. Therefore, cell global identity alone cannot be used to localise the correct position of faulty cell during an outage situation. The detection and localization phase of our COD framework make use of estimated dominance map and reference z-score information established in the profiling phase to detect and localise faulty cell, as discussed in the following subsection.

3.2. Detection and localization phase

In the detection phase, the trained detection model is employed to classify network measurements as normal or anomalous. The output of the detection model allows us to compute a test z-score for each eNB. To establish a correct cell measurement association, the geo-location of each report is correlated with the estimated dominance maps. In this way, we can achieve detection and localization by comparing the deviation of test z-score of each cell with that of reference z-score, as illustrated in Figure 2.

4. CELL OUTAGE COMPENSATION FRAMEWORK

The output of the detection phase is fed into the COC module. This module is based on our previous work combining fuzzy logic and RL algorithm as detailed in [15].

4.1. Fuzzy logic and reinforcement learning

In the proposed COC module, fuzzy logic-based decision mechanism is implemented in contrast to the binary (0,1) decisions that is not always appropriate for applications where a more dynamic and human-like approach is needed. Fuzzy logic induces various degrees of outputs depending on the input conditions. The main benefits of such outputs is that the system can be controlled using linguistic terms such as 'high' or 'low' instead of providing

actual numerical values. Three main components of a fuzzy logic-based system are fuzzification, rule-based inference and defuzzification. Fuzzification is the mapping of crisp input variables to fuzzy sets (linguistic interpretation), rule-based inference is the process of taking decisions based on 'if...then' pre-set rules and, finally, defuzzification process generates quantifiable crisp outputs based on the degree of membership of the outcome in the fuzzy sets. For our specific problem of multiple inputs and multiple outputs with a requirement of degree of membership function, Mamdani-type fuzzy logic is preferred due to its simplicity and suitability for multiple outputs, whereas Sugeno-type fuzzy has a single output without membership functions. Further, we employ the *temporal difference* scheme to solve our problem, as they do not require modelling of the environment dynamics and can be implemented in an incremental fashion [16]. A bisector defuzzification is used, because in a practical network, the antenna down-tilt angles could only be changed with a maximum precision of $1/10^{th}$ of a fraction. So for this purpose, the new parameters for the antenna down-tilt angles of the compensating neighbours could be easily extracted by bisector method.

As for RL, it is a dynamic machine learning mechanism that interacts with the real time changes in the environment. RL algorithm learns from its past experiences (exploitation) and new actions (exploration), unlike supervised learning where the system is explicitly taught. A new action is considered as a *reward*, if it generates a positive result towards the desired objective else the action is considered as *penalty*.

4.2. Compensation phase

In our study, we demonstrate the combination of fuzzy rules in conjunction with RL algorithm for COC. As shown in Figure 1, the objective is to improve the coverage of the identified outage cell. To achieve this, the proposed solution compares the current performance $Perf(X)$ of the outage cell and its neighbours against their previous performance $Perf(X-1)$. This change in performance is closely monitored by the RL in order to select the direction of the fuzzy logic module based on the previous actions. Depending on the fuzzy module rules, antenna down-tilt and transmit powers of the neighbouring potential compensators are changed. After each cycle of action (i.e. change in antenna down-tilt and transmit powers), the new accumulated $Perf(X)$ is compared against the previous $Perf(X-1)$ by the RL algorithm. The antenna down-tilt and transmit power of the compensators are drawn as the membership functions of the fuzzy logic module, and the target is set as the historical performance of the network before outage. Instead of increasing the transmit power of the compensators, higher weightage is given to antenna down-tilt variation. This policy keeps the interference and the energy consumption of the network low. RL modules aid to determine the direction of fuzzy logic module by comparing the current performance with the performance change as a result of previous fuzzy logic iteration. As it is shown in Figure 1, if the change is accessed

as a *reward*, the fuzzy forward module is activated. Likewise, if the change is accessed as a *penalty*, the fuzzy backward module is activated for the next iteration. The fuzzy logic system iteratively reduces the resolution of the change in *action* as the target performance reaches closer to the target performance. This iterative process halts if there is no improvement detected in $Perf(X)$ as compared with $Perf(X-1)$, in either of the fuzzy directions. At this stage, we consider that the algorithm has finalised the best possible compensation parameters for the potential neighbouring cells.

In summary, our COC solution is based on optimising the coverage and capacity of the identified outage zone by changing the gains of antenna via adjusting the down-tilts and downlink transmission powers of the potential neighbour compensating BSs in that plane.

5. SIMULATION RESULTS

In this section, we first demonstrate the detection performance of our COD framework and subsequently show the coverage optimization achieved in the identified outage cell by our COC solution. The aforementioned performance results were obtained under different network load, channel and configuration settings.

5.1. Simulation setup

To simulate the LTE network based on 3GPP specifications, we employ a full dynamic system tool. We set up a baseline reference scenario that consists of 27 eNBs having an inter-site distance (ISD) of 1000 m, with a cell load of 10 users. All of these users are considered as *active users* because they are configured to perform MDT measurements. To model the variations in signal strength due to topographic features in an urban environment, the shadowing is configured to be 8 dB. Normal periodical MDT measurements as well as radio link failure (RLF)-triggered data due to intra-network mobility, reported by UEs to eNBs, are used to construct a reference database for training outage detection models. To simulate a hardware failure in the network, at some point in the simulation, the antenna gain of a BS is attenuated to -50 dBi that leads to a cell outage in a network. The measurements collected from the outage scenario are then used to evaluate the detection and localization performance of the proposed COD framework. In order to evaluate the performance of the compensation module, we identify three neighbouring sectors to compensate for the outage area. The antenna down-tilt and transmission power of the neighbours are adjusted and optimised so as the best possible configuration is set to safeguard UEs in outage. The detailed simulation parameters are listed in Table II. The detection performance of the outage detection models is also examined for different network configurations, obtained by varying the simulation parameter settings including ISD, load and shadowing.

Table II. Simulation parameters.

Parameter	Values
Cellular layout	27 macrocell sites
Inter-site distance	500, 800 and 1000 m
Sectors	3 sectors per cell
User distribution	Uniform random distribution
Path loss	$L[dB] = 128.1 + 37.6 log_{10}(R)$
Antenna gain (normal scenario)	18 dBi
Antenna gain (SC scenario)	−50 dBi
Slow fading std	4, 8 and 12 dB
Simulation length	420 s (1 time step = 1 ms/1TTI)
Control BS Tx power	46 dBm
Data BS Tx power	23 dBm
Horizontal HPBW	70°
Vertically HPBW	6.8°
Antenna pattern [15]	$B_\phi(\phi) = -max(B_\phi, 12.\frac{\phi - \Phi}{\Delta_\phi})$
Network synchronisation	Asynchronous
HARQ	Asynchronous, 8 SAW channels, maximum retransmission = 3
Cell selection criteria	Strongest RSRP defines the target cell
Load	10, 20 and 30 users/cell
MDT reporting interval	240 ms
Traffic model	Infinite buffer
HO margin	3 dB

Parameter estimation and evaluation

The parameter selection for LOFD and OCSVMD is performed using a combination of grid search and CV method as listed in Algorithm 2. Initially, a grid of parameter values is specified that defines the parameter search space. For example, the hyper-parameters of OCSVMD ν and kernel parameter γ are varied from 0 to 1 with 0.05 interval to determine different combinations. Subsequently, for every unique parameter combination C_i, CV is performed as follows: the D_M is divided into training D_{train} and validation dataset D_{val}, and subsequently, performance of the model is evaluated using K-folds approach as shown in Algorithm 2. The value of K is chosen to be 10 in our framework. The performance estimate of the model over K folds is averaged, and iteratively, this process is repeated until all the parameter combinations are exhausted. The C_i yielding the highest performance estimate is selected as an optimal parameter combination for the target model. The value of k_{min} and k_{max} for LOFD is found out to be 5 and 14. In case of OCSVMD, RBF kernel is employed, and the values of the hyper-parameters ν and γ are found out to be 0.3 and 0.25, respectively. Finally, the test data D_{test} from the outage scenario have been used to estimate the performance of the trained models.

In our study, the quality of the target models is evaluated using receiver operating characteristic (ROC) curve analysis. The ROC curve plots the true positive rate or detection rate (DR) (i.e. a percentage of anomalous measurements correctly classified as anomalies) against the false positive rates (i.e. a percentage of normal cell measurements classified as anomalies) at various threshold settings. An area under ROC curve (AUC) metric is used for model comparison, whereas an AUC value of 1 or close to it is an indicator of higher discriminatory power of the target algorithm.

Algorithm 2 Parameter Estimation using CV Method

1: Define parameter combination C_i, $i = 1, \ldots, M$
2: **for** $i = 1, 2, \ldots, M$: **do**
3:     Split the target dataset D_M into K chunks.
4:     **for** $l = 1, 2, \ldots, K$: **do**
5:         Set D_{val} to be the lth chunk of data
6:         Set D_{train} to be the other $K - 1$ chunks.
7:         Train model using C_i, D_{train} and evaluate its performance P_l on D_{val}.
8:     **end for**
9:     Compute average performance P_i over K chunks
10: **end for**
11: **Parameter Selection**: Select C_i corresponding to highest P_i
12: **Performance Estimation**: Evaluate the performance of the model $M(C_i, D_M)$ on D_{test}

5.2. Cell outage detection results

The training database D_M contains pre-processed embedded measurements from the reference scenario as discussed in Section 3.1. The database is subsequently used to model the normal operational behaviour of the network. The database measurement also includes RLF-triggered samples, because even in the reference scenario, UEs experience connection failures due to intra-LTE mobility or shadowing. The test data collected from the outage scenario are used to evaluate the performance of the outage detection models.

The diagnosis process has been tested in 12 scenarios by changing the shadowing, user-density and ISD parameters of the simulation setup as listed in Table II. We have evaluated the detection performance of the OCSVMD and LOFD against every target network configuration. Figure 3(a) illustrates the MDS projection of MDT measurements from the normal and the outage scenario using the baseline network operational settings. It can be observed that the abnormal measurements belonging to SC scenario lie far from the regular training observations. As discussed earlier in Section 3.1, MDS tries to maximise the variance between the data points, and consequently, dissimilar points are projected far from each other, allowing the models to compute a robust dissimilarity measure for outage detection. The goal of OCSVMD is to learn a close frontier delimiting the contour of training observations obtained from the non-outage scenario. In this way, any observation that lie outside of this frontier-delimited subspace (i.e. representative of the normal state of the network) is classified as an anomaly or an abnormal measurement. However, the inlier population (i.e. measurements that lie inside the OCSVMD frontier) is contaminated with RLF events, which ultimately elongates the shape of the learned frontier. As a result, during the detection phase, the observations from the outage scenario exhibiting similarity to RLF-like observations are positioned within the frontier-delimited space as shown in Figure 3(a), and hence wrongly classified as normal. The shape of the learned
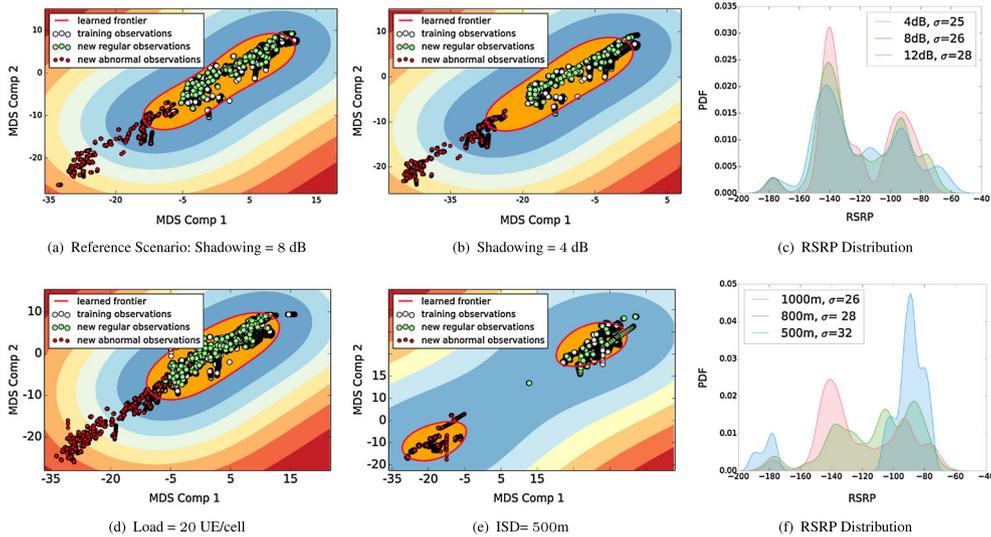
Figure 3. (a) OCSVMD learned network profile for reference scenario, (b) low-shadowing case, (c) distribution of RSRP values for all shadowing cases, (d) medium traffic case, (e) smaller ISD case and (f) distribution of RSRP values for all ISD cases. (a) Reference scenario: shadowing = 8 dB; (b) shadowing = 4 dB; (c) RSRP distribution; (d) load = 20 UE/cell; (e) ISD = 500 m; and (f) RSRP distribution.
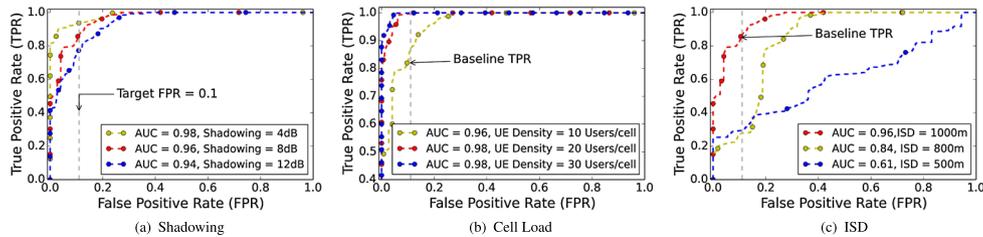

Figure 4. OCSVMD ROC curves for shadowing, traffic and ISD cases. (a) Shadowing, (b) cell load and (c) ISD.

frontier determines the precision of the model for detecting anomalous network measurements.

To study the impact of different radio propagation environment on the detection performance, we varied the shadowing parameter from 8 to 4 dB and 12 dB cases. Under low-shadowing conditions (i.e. 4 dB), it can be observed from Figure 3(b) that inlier population exhibits wider separation from anomalous observation in comparison with reference scenario. This is because higher shadowing conditions affect the spread of the KPI measurements, as indicated in Figure 3(c). It can be inferred from the ROC analysis of OCSVMD that detection performance deteriorates as the shadowing effect is varied from low to high. As shown in Figure 4(a), at target false positive rate of 10 per cent, the model reports the highest DR (i.e. TPR) of 93 per cent under low-shadowing conditions. Likewise, the AUC score has also decreased from 0.98 to 0.94 for high-shadowing scenario (i.e. 12 dB). Moreover, we also analysed the OCSVMD detection performance under varying traffic conditions. Figure 3(d) depicts the distribution of measurements in the MDS space for a user density of 20 per cell. The higher user density implies an increase in the number of training observations that lead to a more accurate estimate of the frontier shape. This explains the slight improvement in the AUC score for OCSVMD with the increase in the cell load as shown in Figure 4(b). A notable DR improvement of 10 per cent is observed for high traffic scenario (i.e. 30 users per cell) in comparison with the baseline OCSVMD.

As for different ISD configurations of a network, we see a significant change in the values of KPI measurements. This is expected because there is a strong correlation between UE reported KPIs and their distance from the eNB. Figure 3(f) shows the distribution of UE reported RSRP values for three different ISD cases. In case of ISD = 500 m, we see a distinct peak of RSRP values around −90 dBm. Likewise, at the farther left end, we see a small peak around −180 dBm that is mainly due to RLF-like observations. In contrast, when ISD = 1000 m, the highest peak value is observed at around −140 dBm, and the observed measurements have lower data spread as indicated in Figure 3(f). As already highlighted, the shape of the learned frontier by OCSVMD is directly affected by the distribution of observations in the embedded space. This becomes evident in Figure 3(e), which shows that the OCSVMD learns two decision frontiers instead of
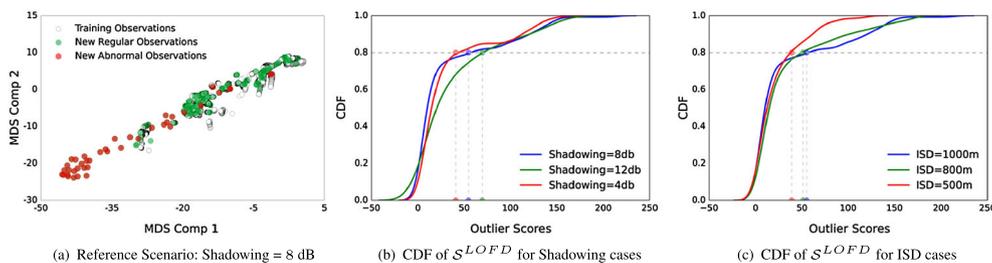
(a) Reference Scenario: Shadowing = 8 dB (b) CDF of $\mathcal{S}^{LOFD}$ for Shadowing cases (c) CDF of $\mathcal{S}^{LOFD}$ for ISD cases

Figure 5. Network profiling using LOFD. (a) Reference scenario: shadowing = 8 dB; (b) CDF of $\mathcal{S}^{LOFD}$ for shadowing cases and (c) CDF of $\mathcal{S}^{LOFD}$ for ISD cases.
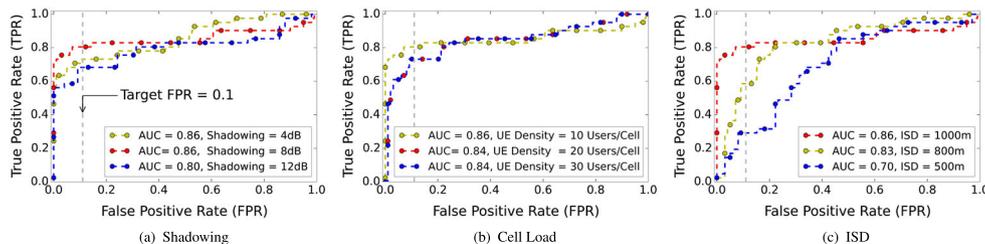

(a) Shadowing (b) Cell Load (c) ISD

Figure 6. LOFD ROC curves for shadowing, traffic and ISD cases. (a) Shadowing; (b) cell load and (c) ISD.

one, because there exists two distinct modes in the data distribution, for the case of ISD = 500 m. As a result, OCSVMD interprets a region where RLF-like event is clustered, as inliers, which leads to an inaccurate network profile. The ROC analysis shown in Figure 4(c) clearly indicates the degradation of OCSVMD performance for lower ISD values.

Similar to OCSVMD, the performance of LOFD is also evaluated for all target network configurations. As explained in Section 3.1, LOFD derives a measure of outlyingness of an observation (i.e. $\mathcal{S}^{LOFD}$), based on the relative data density of its neighbourhood. Figure 5(a) illustrates the labels assigned by LOFD to the observations obtained from the baseline scenario. It can be observed that LOFD classifies some of the test instances that even lie close to the vicinity of training observations as anomalous. Because of such instances, LOFD receives a high outlying scores $\mathcal{S}^{LOFD}$, because the local density around them is highly different from the density of its neighbourhood. To further illustrate the impact of the variation and spread of the data on the values of $\mathcal{S}^{LOFD}$, we plot a cumulative distribution function (CDF) for different shadowing scenarios, as shown in Figure 5(b). It can be seen that for low-shadowing scenario, almost 80 per cent of the observations obtain $\mathcal{S}^{LOFD}$ value less than 50. However, as the shadowing increases, we see a gradual increase in the value of $\mathcal{S}^{LOFD}$. Likewise, a similar behaviour is observed with the increase of ISD, as shown in Figure 5(c). The shadowing and ISD parameters influence the distribution and spread of the data as explained earlier, and consequently the value of $\mathcal{S}^{LOFD}$. This leads to a low detection performance of LOFD, because it generates an increased number of false alarms.
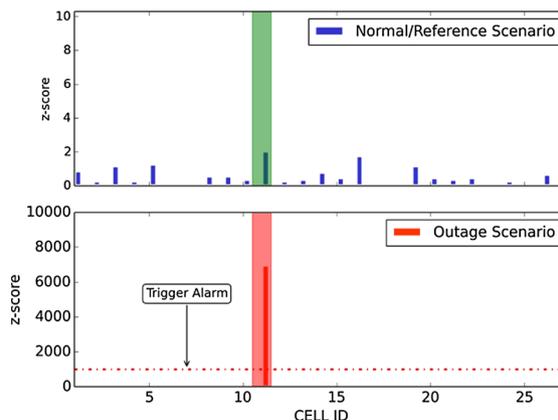

Figure 7. Localization of SC based on per cell z-scores.

As shown in Figure 6(a), the AUC score for LOFD decreases for high-shadowing scenario. On the other hand, the increase in the cell load also increases the spread of the data, which consequently affect the detection performance of LOFD. As shown in Figure 6(b), at false alarm rate of 10 per cent, the highest DR of 81 per cent is achieved for a network scenario in which load configuration is set to be 10 users per cell. Similarly, the change in the ISD has a severe effect on the model performance, and low detection performance of 60 and 30 per cent is achieved for 800 m and 500 m ISD configurations, as shown in Figure 6(c).

In summary, we can conclude from the reported results that OCSVMD under most cases achieves a better detection performance in comparison with LOFD. The outage detection models yield worst performance scores particularly for low ISD network configuration. The performance issue of the target outage detection models can be addressed as follows: for OCSVMD, in the pre-processing
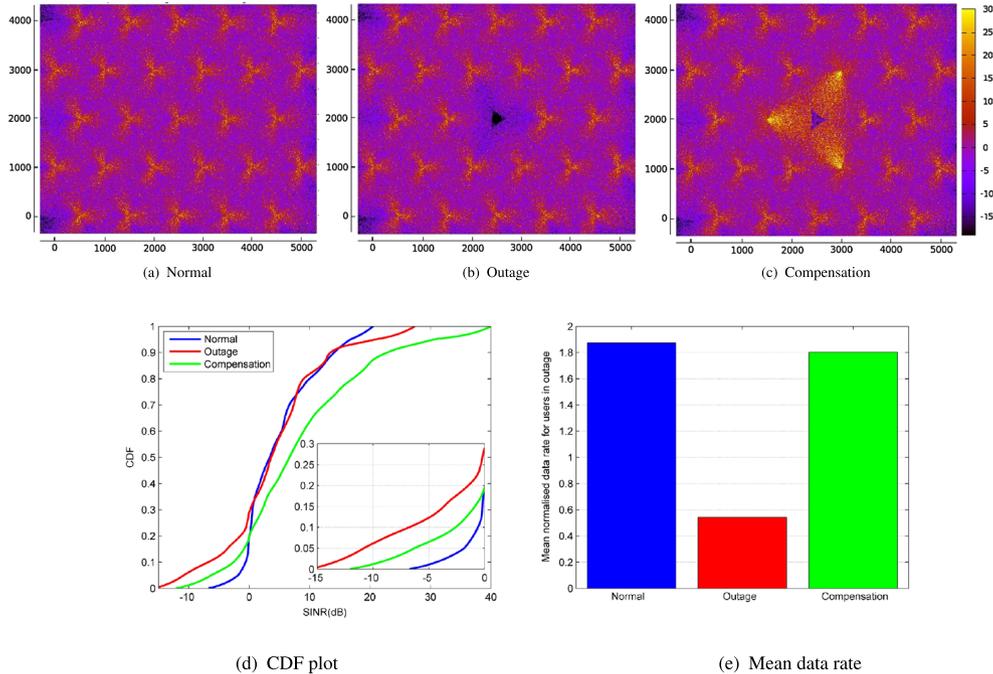
(a) Normal   (b) Outage   (c) Compensation

(d) CDF plot   (e) Mean data rate

Figure 8. Radio environment maps and SINR CDF for normal, outage and compensated case. (a) Normal; (b) outage; (c) compensation; (d) CDF plot and (e) mean data rate.

step, the RLF-like events must be filtered before constructing a training database. This would help decrease the spread of the data and the model would only learn frontier that corresponds to normal operational network behaviour. In case of LOFD, incremental drift detection schemes can be incorporated to re-tune the model parameters in order to minimise the false alarm rate.

5.3. Localization

Because OCSVMD model has outperformed LOFD for most test cases, it has been selected as a final model to compute per cell z-scores for the normal and SC scenario, as shown in Figure 7. It can be observed from Figure 7 that measurements are classified as anomalous even in the normal operational phase of the network due to occurrence of RLF events. This is particularly true for cell ID 1, 5, 11, 16 and 19 whose n_b values are found to be 700, 2000, 3000 and 1500, respectively, in the reference scenario. However, during an outage scenario, because cell 11 is configured as a faulty cell, the corresponding z-scores are significantly higher than the rest of the network. A simple decision threshold can be applied on the computed z-scores to autonomously localise faulty cells, and consequently, an alarm can be triggered. In addition to cell outage localization, the change in the z-score can be used to identify performance degradation issues or a weaker coverage problems. This information can act as an input to self-healing block of SON engine, which can then trigger automated recovery process.

5.4. Compensation

Plot shown in Figure 8(a)–(c) presents the radio environment maps for the normal, outage and compensated cases, respectively, and the colour bar shows the SINR levels. As the subject cell site goes into outage, it is visible that the coverage area of the outage cell has very low SINR levels (depicted in Figure 8(b)), and consequently, the UEs in this low SINR region are susceptible to outage (failure of link to the network). The compensator module optimises the antenna down-tilt and transmit powers of the three potential neighbours such that the coverage gap is filled. It is visible from radio environment map in Figure 8(c) that SINR of outage region is significantly improved after compensation.

Figure 8(d) presents the comparison of SINR levels with a CDF plot for the target region in and around the outage cell. It is visible from the zoomed figure that in the outage case, there are several UEs in the low SINR region. However, after compensation, there is a significant reduction in the percentile of users in the low SINR region. Another visible effect is that in the compensation case, a majority of the UEs also have substantially high SINR levels. This is due to the fact that the increase transmit power and change in antenna down-tilt configuration further improves the SINR performance of the UEs closer to the compensating neighbours.

We also present in Figure 8(e) the bandwidth normalised data rate performance of the UEs present in the outage area. It is evident that the mean data rate performance of the UEs is significantly reduced in case of an outage. However,

as the compensation is applied, the coverage of the identified outage area is optimised relatively close to the normal conditions.

6. CONCLUSION

This paper has presented a data-driven analytics framework for autonomous outage detection and coverage optimization in an LTE network, which exploits the minimization of drive test functionality as specified by 3GPP in Release 10. The outage detection approach first learns a normal profile of the network behaviour by projecting the network measurements to low-dimensional space. For this purpose, multi-dimensional scaling method in conjunction with domain and density-based detection models, OCSVMD and LOFD, respectively, was examined for different network conditions. It was established that OCSVMD, a domain-based detection model attained a higher detection accuracy compared with LOFD, which adopts a density-based approach to identify abnormal measurements. Finally, the UE reported coordinate information is employed to establish the dominance areas of target cells that are subsequently used to localise the position of outage zone. To optimise the coverage and capacity of the identified outage zone, a fuzzy-based RL algorithm for COC is proposed. The COC algorithm achieves coverage optimization by adjusting the gains of the antennas through antenna down-tilt and downlink transmission power of the neighbouring BSs. Simulation results have shown that the COC algorithm can recover a significant number of UEs from outage.

ACKNOWLEDGEMENT

REFERENCES

1. Aliu OG, Imran A, Imran MA, Evans B. A survey of self organisation in future cellular networks. *IEEE Communications Surveys & Tutorials* 2013; **15**(1): 336–361.
2. Hämäläinen S, Sanneck H, Sartori C. *LTE Self-Organising Networks (SON): Network Management Automation for Operational Efficiency*. John Wiley & Sons: Chichester, 2012.
3. Mueller CM, Kaschub M, Blankenhorn C, Wanke S. A cell outage detection algorithm using neighbor cell list reports. In *Self-Organizing Systems*. Springer: Berlin Heidelberg, 2008; 218–229.
4. Liao Q, Wiczanowski M, Stanczak S. Toward cell outage detection with composite hypothesis testing. In *IEEE ICC*, Ottawa, Canada, 2012; 4883–4887.
5. Barco R, Wille V, Díez L. System for automated diagnosis in cellular networks based on performance indicators. *European Transactions on Telecommunications* 2005; **16**(5): 399–409.
6. Cheung B, Fishkin SG, Kumar GN, Rao SA. Method of monitoring wireless network performance. *US Patent App.* 10/946, 255, 2004.
7. Ma Y, Peng M, Xue W, Ji X. A dynamic affinity propagation clustering algorithm for cell outage detection in self-healing networks. In *Proceedings of IEEE Wireless Communications and Networking Conference (WCNC)*, Shanghai, China, 2013; 2266–2270.
8. Khanafer RM, Solana B, Triola J, Barco R, Moltsen L, Altman Z, Lazaro P. Automated diagnosis for UMTS networks using Bayesian network approach. *IEEE Transactions on Vehicular Technology* 2008; **57** (4): 2451–2461.
9. Coluccia A, DAlconzo A, Ricciato F. Distribution-based anomaly detection via generalized likelihood ratio test: A general maximum entropy approach. *Computer Networks* 2013; **57**(17): 3446–3462.
10. Razavi R, Klein S, Claussen H. A fuzzy reinforcement learning approach for self-optimization of coverage in LTE networks. *Bell Labs Technical Journal* 2010; **15**(3): 153–175.
11. Dirani M, Altman Z. Self-organizing networks in next generation radio access networks: Application to fractional power control. *Computer Networks* 2011; **55**(2): 431–438.
12. Cox TF, Cox MA. *Multidimensional Scaling*. CRC Press: Florida, USA, 2010.
13. Breunig MM, Kriegel HP, Ng RT, Sander J. LOF: identifying density-based local outliers. *ACM Sigmod Record* 2000; **29**: 93–104.
14. Schölkopf B, Platt JC, Shawe-Taylor J, Smola AJ, Williamson RC. Estimating the support of a high-dimensional distribution. *Neural Computation* 2001; **13**(7): 1443–1471.
15. Saeed A, Aliu O, Imran M. Controlling self healing cellular networks using fuzzy logic. In *IEEE Wireless Communications and Networking Conference (WCNC)*, Shanghai, China, 2012; 3080-3084.
16. Razavi R, Claussen H. Improved fuzzy reinforcement learning for self-optimisation of heterogeneous wireless networks. In *20th International Conference on Telecommunications (ICT)*, Casablanca, 2013; 1–5.